Title
Distribution of the calcium-binding protein SPARC in tissues of embryonic and adult mice.

Journal
Journal of Histochemistry & Cytochemistry, 37(6)

ISSN
0022-1554

Authors
Sage, H
Vernon, RB
Decker, J
et al.

Publication Date
1989-06-01

DOI
10.1177/37.6.2723400

Peer reviewed

0022-1554/89/$3.30
The Journal of Histochemistry and Cytochemistry
Vol. 37, No. 6, pp. 819-829, 1989
Printed in U.S.A.

Original Article

Distribution of the Calcium-binding Protein SPARC In Tissues of Embryonic and Adult Mice[1]

HELENE SAGE,[2] ROBERT B. VERNON, JAY DECKER, SARAH FUNK, and MARIA LUISA IRUELA-ARISPE

Department of Biological Structure, University of Washington, Seattle, Washington 98195.

Received for publication August 29, 1988 and in revised form December 20, 1988; accepted December 27, 1988 (8A1470).

SPARC (Secreted Protein that is Acidic and Rich in Cysteine), a Ca^{++}-binding glycoprotein also known as osteonectin, is produced in significant amounts by injured or proliferating cells in vitro. To elucidate the possible function of SPARC in growth and remodeling, we examined its distribution in embryonic and adult murine tissues. Immunohistochemistry on adult mouse tissues revealed a preferential association of SPARC protein with epithelia exhibiting high rates of turnover (gut, skin, and glandular tissue). Fetal tissues containing high levels of SPARC included heart, thymus, lung, and gut. In the 14–18-day developing fetus, SPARC expression was particularly enhanced in areas undergoing chondrogenesis, osteogenesis, and somitogenesis, whereas 10-day embryos exhibited selective staining for this protein in Reichert's membrane, maternal sinuses, and trophoblastic giant cells. SPARC displayed a Ca^{++}-dependent affinity for hydrophobic surfaces and was not incorporated into the extracellular matrix produced by cells in vitro. We propose that in some tissues SPARC associates with cell surfaces to facilitate proliferation during embryonic morphogenesis and normal cell turnover in the adult. (*J Histochem Cytochem 37:819–829, 1989*)

KEY WORDS: SPARC; Calcium binding; Mouse embryo; Morphogenesis; Trophoblast.

Introduction

SPARC is a secreted Ca^{++}-binding protein which is induced in conjunction with cell differentiation, proliferation, stress, and certain developmental signals (Holland et al., 1987; Mason et al., 1986a,b; Sage et al., 1986). Molecular cloning and protein sequence analysis have shown that SPARC is identical to osteonectin (ON), originally described as a major noncollagenous protein of bone which bound Ca^{++}, hydroxyapatite, and type I collagen (Bolander et al., 1988; Mason et al., 1986b; Young et al., 1986; Romberg et al., 1985; Termine et al., 1981). SPARC is also identical to BM-40, a product of a basement membrane-secreting tumor cell line (Mann et al., 1987; Dziadek et al., 1986), and to an M_r 43 KD glycoprotein, synthesized in vitro by cells of the vessel wall as well as by other normal and transformed cells derived from all primordial germ layers (Sage et al., 1981, 1984). ON was also found in dentin, periodontal ligament (Tung et al., 1985), and platelets (Stenner et al., 1986), and was a synthetic product of gingival and ligament fibroblasts (Zung et al., 1986; Wasi et al., 1984) and calvarial cells in vitro (Otsuka et al., 1984). The M_r 43 KD protein was identified as a "culture shock" protein which bound bovine serum albumin (BSA) and a 70 KD serum protein, and which was associated with endothelial cell migration, proliferation, serum deprivation, and endotoxin-mediated injury (Sage, 1986a; Sage et al., 1986).

Since bone ON/SPARC is now known to be a potent inhibitor of hydroxyapatite formation (Romberg et al., 1985), it has been suggested that the protein might inhibit (Engel et al., 1987) rather than promote (Termine et al., 1981) extracellular mineralization. Although SPARC mRNA levels are decreased in virally transformed cells (Mason et al., 1986a; Young et al., 1986), it has been observed that SPARC is up-regulated in normal cells undergoing proliferation (Sage et al., 1986). The location of SPARC protein in vivo, however, has remained controversial. By immunofluorescence histochemistry, ON has been identified in the extracellular matrix and in cells of ligament and mineralizing tissues (Tung et al., 1985; Wasi et al., 1984; Termine et al., 1981), while BM-40 was observed in a limited number of basement membranes (Dziadek et al., 1986). In contrast, SPARC mRNA has been localized in a variety of tissues. A recent study has shown tissue-specific and developmentally related expression of SPARC mRNA in fetal and adult mice (Holland et al., 1987). These results suggested the association of SPARC with proliferating cells in several tissues.

In this study we developed highly specific polyclonal antibodies to examine the distribution of SPARC protein in embryonic and adult mice. Its association with morphogenesis and proliferation in certain tissues resembled in part the immunohistochemical distribution of TGF-β protein in the mouse embryo (Heine et al., 1987). We have also shown that SPARC has a Ca^{++}-sensitive affinity for

[1] Supported by NIH grant HL18645.
[2] To whom correspondence should be addressed.

hydrophobic surfaces. SPARC may therefore function as an extracellular modulator of Ca^{++} at the cell surface which either initiates or facilitates cell migration and/or growth.

Materials and Methods

Cell Culture

Human femoral head osteoblasts in primary culture were a gift from Dr. W. Lanzer (University of Washington). MG63 human osteosarcoma cells were obtained from American Type Culture Collection (Rockville, MD). Mouse PYS-2 cells, a teratocarcinoma line derived from parietal yolk sac endoderm, were gifts from Drs. B. Hogan (Vanderbilt University, Nashville, TN) and J. Lehman (Albany Medical College, Albany, NY). Metabolic labeling of cells in vitro with [^{35}S]-Met was according to Sage et al. (1986) and Sage (1986a).

Purification of SPARC Protein

PYS-2 cells were primarily used as a source of SPARC. Subconfluent cells ($15–20 \times 10^6$) were incubated in Dulbecco Modified Eagle's Medium (DMEM) in the absence of fetal calf serum; 21 hr later the medium was collected, clarified of cell debris, and stirred overnight at 4°C in the presence of 50% (w/v) ammonium sulfate. The precipitated protein was pelleted by centrifugation, dissolved in and dialyzed against a 4 M urea–50 mM Tris-HCl buffer (pH 8), and chromatographed on diethylaminoethyl (DEAE)-cellulose at 4°C. The flow-through was discarded; laminin and BSA were eluted both with 75 mM and 175 mM NaCl in the same buffer, and SPARC was eluted with 175 mM NaCl (Sage et al., 1984, 1986). Dialysis of this second eluate peak against distilled water caused SPARC to precipitate quantitatively, while the BSA remained in solution. This precipitation occurred in a relatively narrow pH range (3.5–5.5) and could be inhibited by 10 mM ethylenediamine tetraacetic acid (EDTA). SPARC was purified further by chromatography on Sephadex G-200 in Tris-buffered saline (TBS) at 4°C or, alternatively, by carboxymethyl (CM)-cellulose chromatography at 20°C in a 2 M urea, 40 mM Na acetate buffer (pH 4.5), after an initial denaturation step at 40°C for 5–10 min. Pure SPARC (250–500 μg) was recovered from 50×10^6 PYS cells. To monitor the purification, one dish of cells was often radiolabeled with [^{35}S]-Met. However, SPARC used for Western blotting was nonradioactive.

Sodium dodecylsulfate polyacrylamide gel electrophoresis (SDS-PAGE), protein staining, fluorescence autoradiography, and scanning densitometry were performed as previously described (Sage et al., 1986; Laemmli, 1970).

Preparation and Characterization of Antibodies

Both native SPARC (purified on G-200) and denatured SPARC (purified on CM-cellulose) were used to generate polyclonal antibodies in adult rabbits. IgG was precipitated from whole antisera by addition of ammonium sulfate to a final concentration of 20% (w/v). IgG specific for SPARC was purified by affinity chromatography on Sepharose CL-4B (Pharmacia; Piscataway, NJ) coupled with purified SPARC, according to the manufacturer's instructions. Affinity-purified anti-SPARC IgG (typical concentrations ranged from 0.1–0.225 mg/ml) was reactive by enzyme-linked immunosorbent assay (ELISA) at dilutions in excess of 1:2048 and exhibited no reactivity towards BSA or fetal calf serum. Antibodies were characterized by ELISA, Western blotting, and radioimmune precipitation (Sage et al., 1984, 1986).

Proteins were transferred to nitrocellulose for 1–3 hr at 500 mA, stained with Amido black, de-stained, and blocked in 1% non-fat dry milk–0.05% Tween in PBS at pH 8.0 (MT buffer), with gentle shaking at room temperature for 1–2 hr or at 4°C overnight. Anti-SPARC antisera (diluted at a minimum of 1:1000) or affinity-purified antibodies (diluted 1:250–500) were incubated with the blot in MT buffer overnight at room temperature. The blot was subsequently washed five times for 5 min each in MT buffer, incubated 2–3 hr with 100 μl [^{125}I]-protein A (approximately 10 μCi) (New England Nuclear; Boston, MA) in 35 ml MT buffer, washed sequentially in 1% MT buffer (twice for 10 min) and PBS-Tween (eight times, for a minimum of 2 hr), and dried before exposure to X-ray film.

Structural Studies and Binding Assays

Circular Dichroism. Far ultraviolet circular dichroism spectra were obtained at 20°C from a Cary 61 spectrometer, calibrated with D(−)-panto-

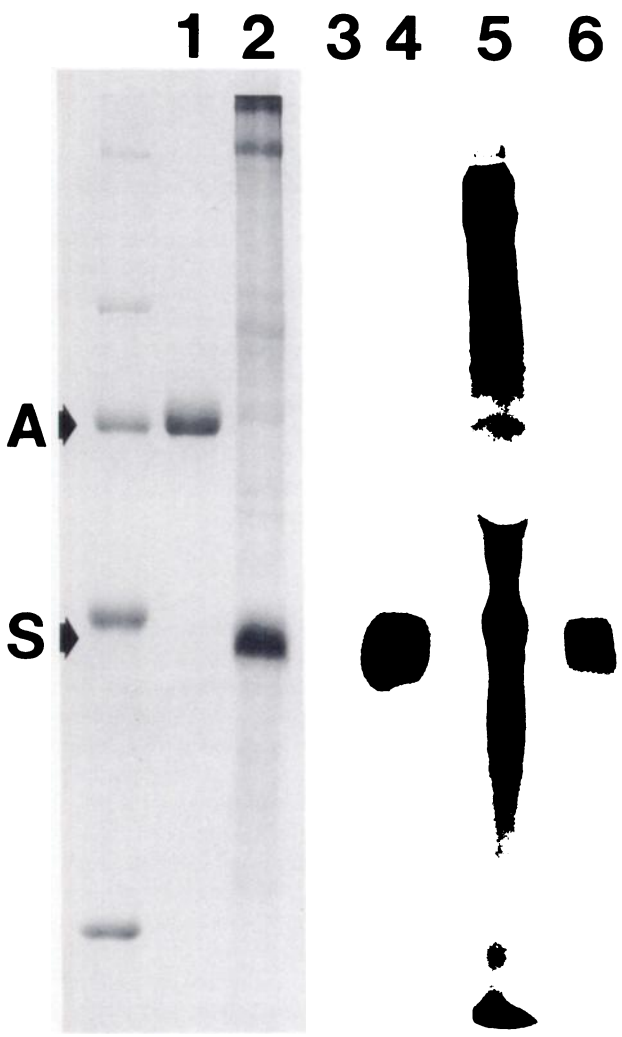

Figure 1. Fractionation and identification of SPARC in PYS culture media. Serum-free culture media were collected from subconfluent PYS cells. Lanes **1** and **2** show Coomassie blue-stained proteins, fractionated initially by ammonium sulfate precipitation and DEAE-cellulose chromatography, which were dialyzed against water at pH 5.5. Lane **1** (supernatant) contains BSA (A) and lane **2** (precipitate) contains primarily SPARC (S). Western blotting of lane **2** material with affinity-purified anti-SPARC IgG in conjunction with [^{125}I]-protein A is shown in lane **4**; lane **3** is a duplicate sample incubated with antibody that was pre-absorbed with SPARC. [^{35}S]-Met-labeled proteins secreted by PYS cells (lane **5**) yield purified SPARC after immunoprecipitation with anti-SPARC IgG (lane **6**). Proteins in the presence of DTT were resolved by SDS-PAGE on 5%/10% gels. Molecular weight markers, shown on the far left, are, in descending order, 200 KD, 97 KD, 68 KD, 43 KD, and 28 KD.

lactone, with a quartz cell of 0.1-mm path length. Protein concentrations ranged from 0.15–0.45 mg/ml (5.1–15 μM) in TBS containing 2.5–5 mM $CaCl_2$ or 12 mM EDTA. The molar ellipticity θ at 220 nm (deg cm^2/dmol) was calculated from a mean residue molecular weight of 110 determined from the amino acid composition of murine SPARC (Mason et al., 1986b). Protein concentration was determined by amino acid analysis (performed by Dr. D. Eyre, University of Washington) or from an extinction coefficient ($E^{0.1\%}$/280, 1 cm) of 1.076 calculated from the compositional data and the molecular weight of 33,062 predicted from the cDNA sequence (Mason et al., 1986b).

Chelex Ca^{++}-binding Assay. This procedure followed closely the methodology described by Waisman et al. (1986) and Waisman and Rasmussen (1983). Chelex 100 (minus 400 mesh; Bio-Rad, Richmond, CA)-treated buffers were used throughout the four separate experiments. In a typical set, 249.3 μg (7.54 nmol) of purified native SPARC was dissolved in 100 μl 100 mM Tris-HCl, pH 7.4–50 mM NaCl buffer. Purified bovine testicular calmodulin (a gift from Dr. R. Klevit, University of Washington) at a similar concentration was examined for ^{45}Ca-binding activity in parallel with SPARC. To 25 μl Chelex resin were added various amounts (10–150 μl) of SPARC or calmodulin and from 1–25 μl [^{45}Ca]-Cl_2 (2 mCi or 93 μg Ca/ml; Amersham International, Poole, UK), in a final volume of 500 μl Chelexed buffer. Solutions were vortexed frequently, microfuged, and 2–100 μl aliquots of the supernatant were counted by liquid scintillation spectrometry (Waisman et al., 1986). In each set of experiments, the ionic strength was kept at a constant value. Controls included BSA and reaction mixtures without protein. Protein concentrations were determined by amino acid analysis.

Affinity Chromatography

Metal chelate affinity chromatography (iminodiacetic acid coupled to epoxy-activated Sepharose 6B; Pharmacia) was performed according to the manufacturer's instructions. The column was equilibrated in $CuSO_4$ (2.5 mg/ml) and samples were eluted with 0.05 M EDTA–0.5 M NaCl, followed by 2 M EDTA, pH 7.0, and 1% SDS. Phenyl Sepharose chromatography (Pharmacia) was according to Davis et al. (1986) with modifications as described in the figure legend.

Immunohistological Studies

Immunofluorescence microscopy was performed on cells grown on glass coverslips in vitro as previously described (Sage et al., 1984, 1986). Antibody concentrations were determined by absorbance at 280 nm and extrapolation to a standard curve for normal rabbit IgG.

Timing of mouse embryos was as follows: females were injected with pregnant mare serum at 1700 hr the first day and human chorionic gonadotropin at 1700 hr on the second day; midnight on the following (third) day (24 hr after appearance of the vaginal plug) marked the end of day 1.

Tissues and embryos from Swiss-Webster mice were either frozen immediately after dissection in OCT (Tissue-Tek) in liquid N_2-cooled Freon 12 or immersed for 4–6 hr in Bouin's fixative (0.9% picric acid and 9% formaldehyde by volume in 5% acetic acid). Some of the fixed specimens were demineralized in 8 N formic acid: 1 N Na formate (1:1) for 12–18 hr. Fixed tissues were dehydrated in ascending concentrations of ethanol, cleared in toluene, and embedded in paraffin. Sections were cut at a thickness of 6 μm (paraffin blocks) or 8 μm (cryostat sections) and were placed on slides pre-coated with a 0.1% solution of poly-L-lysine in water. Paraffin sections were dried overnight at 41°C and stored at −20°C for a maximum of 1 week before use. Paraffin sections were deparaffinized in two washes (5 min each) of xylene, rehydrated through a graded series of ethanol solutions to 70%, and washed four times for 3 min in PBS. Frozen sections were fixed for 5 min in 2% paraformaldehyde at 4°C and were dried for 0.5 hr at 24°C (Sage et al., in press).

Sections intended for immunoperoxidase staining were incubated 30 min in 70% methanol containing 3% H_2O_2, followed by PBS, to inactivate endogenous peroxidases. Nonspecific binding of immunoglobulins was minimized by incubating sections in PBS–10% normal goat serum. Sections were exposed sequentially to anti-SPARC IgG, diluted in 1% normal goat serum–PBS (dilutions varied with the titer of the antibody, as determined by ELISA, and were generally from 1:50–100 for ammonium sulfate precipitates and 1:2–5 for affinity-purified fractions), and rhodamine- or fluorescein isothiocyanate (RITC, FITC)-conjugated to goat antibodies against rabbit IgG (diluted 1:100 in 10% goat serum) (Sage et al., in press). Alternatively, sections were exposed sequentially to anti-SPARC IgG, biotinylated goat antibodies against rabbit IgG, avidin–biotin–peroxidase complex (ABC Reagent; Vector Labs, Burlingame, CA), and 3,3'-diaminobenzidine–4 HCl (3 mg/ml in 0.05 M Tris-HCl, pH 7.6, containing 0.02% H_2O_2) (8–10 min). Sections were washed in PBS (four times for 3 min) after each addition. Kodak Tri-X film was used for black-and-white photography, Kodak 50T type EPY was used for brightfield color photomicroscopy, and Kodak ASA 400 Ektachrome was used for color photography with a Zeiss Photomicroscope equipped for epifluorescence. Specificity controls included (a) substitution of normal rabbit IgG at the same concentration used for anti-SPARC IgG, (b) use of second antibody alone, (c) incubation of primary antibody with excess purified SPARC or BSA, (d) use of a series of concentrations of several preparations of primary antibody, and (e) use of rabbit anti-human plasma fibronectin (FN) IgG (a gift from Dr. P. Bornstein, University of Washington) on serial sections.

Results

Previous studies by others and from our own laboratory had shown SPARC to be secreted by cells derived from all germ layers under a variety of culture conditions. A common observation was the association of SPARC with cells undergoing proliferation, migration, attachment or detachment, and modulation of biosynthetic phenotype in response to a foreign substrate and/or factors present in serum (Sage, 1986a,b). In an effort to understand the function of this protein in vivo, we produced antibodies to murine SPARC and examined its distribution in fetal and adult mice. As shown in Figure 1 (lane 4), polyclonal affinity-purified anti-SPARC IgG reacted on a Western blot specifically with SPARC protein. Lanes 1 and 2 of Figure 1 show that dialysis of the 175 mM NaCl eluate against water (pH 5.5) caused SPARC to precipitate (lane 2), while the major contaminant, BSA, remained in the supernatant (lane 1). This behavior of SPARC, which is Ca^{++} dependent, is probably owing to the acidic pI of the protein, 4.3 (Mason et al., 1986b). The protein fraction shown in lane 2 was further purified by native chromatography on Sephadex G-200 or under denaturing conditions (which resulted in higher yields) on CM-cellulose. These preparations contained a single M_r 43,000 component (shown in later figures) which was used for affinity purification of anti-SPARC IgG and for absorption of the antibody as a specificity control (as shown in Figure 1, lane 3). Radioimmune precipitation of [^{35}S]-Met-labeled PYS cell culture medium protein (lane 5) produced a single species of M_r 43,000 (lane 6).

In earlier studies we had shown that SPARC (as 43 KD protein) was not incorporated in vitro into the extracellular matrix of BAE cells, smooth muscle cells, fibroblasts (Sage et al., 1981, 1986), or parietal endoderm (Mason et al., 1986b). However, in view of recent reports which have proposed a basement membrane- or matrix-

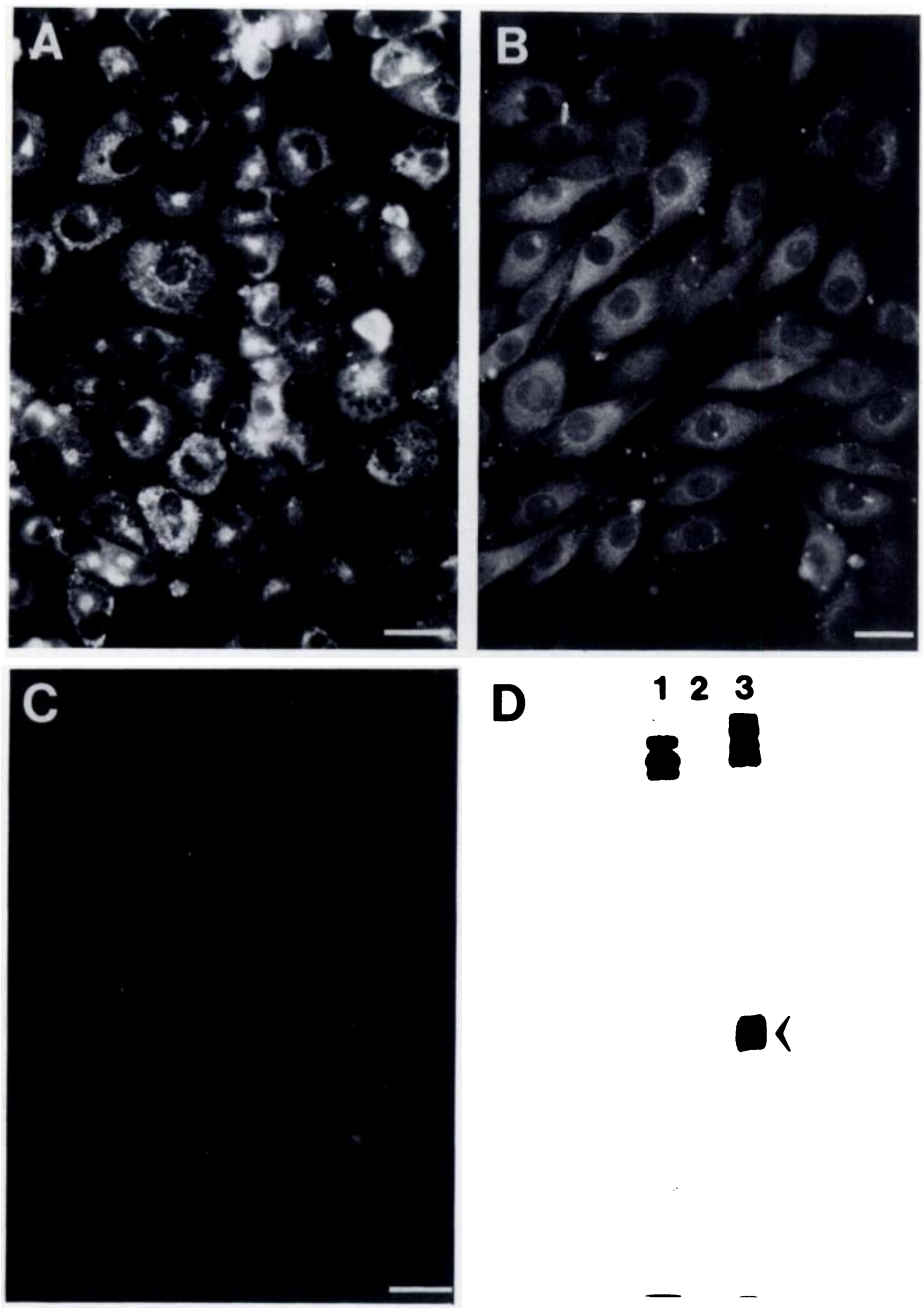

Figure 2. Localization of SPARC protein in vitro. PYS (**A**) and human osteosarcoma cells (**B,C**) were permeabilized and exposed to anti-SPARC IgG (**A,B**) or to antibody preabsorbed with SPARC (**C**), followed by FITC–secondary antibody. Both cells exhibited cytoplasmic vesicular staining, with no reactivity in the extracellular matrix. Proteins secreted from human osteoblasts labeled with [^{3}H]-Pro were fractionated on DEAE-cellulose and resolved by SDS-PAGE on a 5%/10% gel under reducing conditions. Lanes **1–3** denote step gradient fractions eluted from the column of 0, 75, and 175 mM NaCl, respectively. Arrowhead identifies SPARC at M_r 43,000. Original magnifications: **A–C** × 250. Bars = 25 μm.

associated role for this protein (Mann et al., 1987; Tung et al., 1985; Termine et al., 1981), we examined the distribution of SPARC in PYS cells and a human osteosarcoma-derived cell line, MG63. As shown in Figures 2A and 2B, immunoreactive SPARC protein was confined to cytoplasmic granules of these permeabilized cells. Despite a significant level of SPARC in the medium from MG63 cell cultures (Figure 2D, lane 3), SPARC protein was noticeably absent from the spaces between or under the cells. Figure 2C shows that pre-incubation of the antibody with SPARC protein completely inhibited the staining reaction.

SPARC Is Associated with Certain Proliferating Cells and with Morphogenic Processes During Embryogenesis

We examined the distribution of SPARC protein in fetal, newborn, and adult mouse tissues by immunofluorescence and immunoperoxidase staining with affinity-purified anti-SPARC IgG. Reactivity of the antibody preparations was highest on frozen sections and lowest on paraffin-embedded tissue fixed in paraformaldehyde. Tissue fixed in Bouin's solution, on the other hand, retained antige-

Table 1. *Distribution of SPARC protein in mouse*

	Fetus[a]	Adult
Alimentary tract		
Tongue	+	+
Oral epithelium	+	
Esophagus	+	+
Stomach		+
Small intestine	+	+
Glandular Tissue		
Submaxillary gland		+
Parotid gland		+
Adrenal gland	−	−
Pancreas	−	−
Mammary gland		+
Thymus	+	−
Muscle and Nerve		
Skeletal muscle (tongue, diaphragm)	+	+
Olfactory nerve		+
Somites	+	
Cartilage and Bone		
Calvaria, including epithelium	+	
Vertebrae (chondrocytes and perichondrium)	+	
Osteoid/osteoblasts	+	
Sagittal sutures of skull	+	
Marrow	+	+
Reproductive Tissue		
Ovary		+
Testis		+
Epididymis		+
Other Organs		
Heart	+	−
Liver	−	−
Kidney	−	−
Lung	+	−
Spleen		−
Skin	+	+

[a] Tissues were from 14–18-day embryos; chondrogenic tissue from 12-day embryos was also positive.

nicity towards anti-SPARC IgG and had better morphology. Results of this tissue survey are presented in Table 1; the distribution of SPARC in newborn mouse was similar to that seen in the adult and was therefore not included. In most cases, both frozen and Bouin's-fixed tissues were examined by RITC- and/or FITC-based immunofluorescence and by immunoperoxidase staining, with a minimum of two different antibody preparations. The distribution of SPARC in the respective tissues under these various experimental conditions was nearly coincident. All tissues were checked for autofluorescence and reactivity towards anti-FN and normal rabbit IgG.

To further confirm the specificity of the affinity-purified anti-SPARC polyclonal antibodies, we first tested the preparation on sections of 10 day mouse embryos. As shown in Figures 3A and 3B, a positive reaction was observed in the cells of the parietal endoderm that secrete Reichert's membrane. Trophoblastic giant cells and endothelia lining the maternal sinuses also exhibited a strong staining reaction indicative of the presence of SPARC (Figures 3B–3D).

Representative tissues from embryonic and newborn mice are shown in Figures 4 and 5. Alveolar epithelium (and probably endothelium), as well as ductal epithelium, stained positively for SPARC in 18-day fetal lung (Figure 4A); this tissue, however, was negative in the adult (Table 1). Thoracic (and caudal, not shown) somites from 14-day embryos expressed SPARC antigen (Figure 4B). In developing bone, SPARC was localized primarily to the perichondrium/periosteum in 18-day embryos (Figure 5A), but a more generalized distribution was seen in newborn (4–5-day) long bone, where SPARC was associated with nonhypertrophic chondrocytes (Figure 5B). In the newborn, staining for SPARC was also seen in periosteum and perichondrium, and in association with osteoblasts and newly synthesized osteoid (Figure 5C). Chondrogenic tissues from 12-day embryos were also positive for SPARC (Table 1, footnote); however, tongue and intestine from these animals were negative.

Some of the other tissues listed as positive for SPARC in Table 1 are shown in Figure 6. SPARC was clearly associated with proliferating epithelia in several tissues. In Figure 6A, the epidermal covering of newborn skull stained intensely with anti-SPARC IgG; for comparison, anti-FN IgG identified antigen in the connective tissue interstitium of the skin (Figure 6B). In newborn thymus, SPARC was associated with the epithelial processes that provide support for T-cell populations (Figure 6C). At this stage of development, both epidermal and thymic epithelial cells are undergoing generalized proliferation. In lactating mammary gland, SPARC was associated with both the ductal and alveolar epithelia that proliferate in response to hormonal stimuli during late stages of the reproductive cycle (Figure 6D).

Anti-SPARC antibodies consistently did not stain the extracellular matrix of many different cell types in vitro (Sage et al., 1986) (Figure 2). Therefore, it appears that SPARC protein visualized by immunostaining in vivo (Figures 3–6) was located primarily in the cells. Additional explanations are that SPARC was closely apposed to the surface of the cell that secreted it, was bound to a component of the interstitium, or was immobilized by the fixation procedure en route to another destination.

The presence of SPARC in mesenchymal cells (e.g., chondrocytes, osteoblasts, osteo- and fibroprogenitor cells of the perichondrium, somitic cells), as well as cells derived from primitive ectoderm (pneumocytes, thymic epithelium) and extra-embryonic (parietal) endoderm (Mason et al., 1986a,b), is suggestive of a generalized rather than a lineage-specific function in cell behavior. In some cases this function may be related to proliferation or migration, as seen in certain embryonic tissues but not in their adult counterparts (e.g., thymus, heart, lung). SPARC is present in adult tissues that exhibit high rates of proliferation (e.g., gut mucosa, salivary gland) (Table 1). However, both the temporal and spatial restriction of SPARC in the mouse suggests that expression of the protein, although not lineage-specific, may be related to certain stages of cell differentiation and/or cell cycle.

Calcium-binding Properties of SPARC

The amino acid sequence predicted from mouse SPARC cDNA revealed two putative Ca^{++}-binding domains—a unique, acidic, Glu-rich N-terminal region (Domain I), and an EF-hand-containing region (Domain IV) which is homologous to Ca^{++}-binding loops in calmodulin (Engel et al., 1987). An additional EF-hand has been

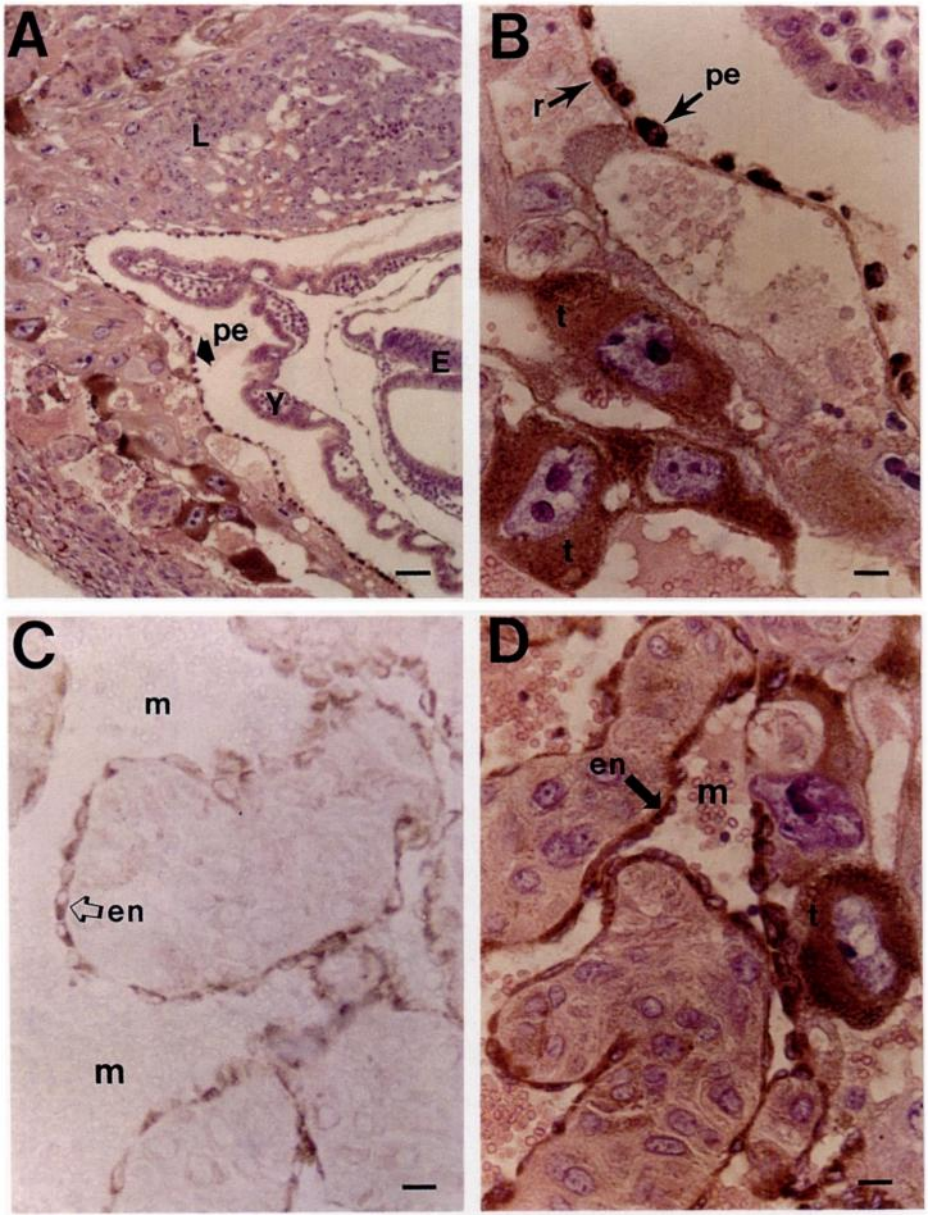

Figure 3. Distribution of SPARC in the 10-day mouse embryo. Paraffin sections of Bouin's-fixed 10-day mouse embryo and placenta were exposed to anti-SPARC IgG and specific immune complexes were visualized by avidin–biotin–peroxidase method. Sections were counterstained with hematoxylin and eosin. (**A**) Embryo (E) surrounded by the visceral yolk sac (Y), as well as parietal endoderm (pe) and the placental labyrinth (L). Brown diaminobenzidine reaction product, indicating presence of SPARC, was seen in the parietal endoderm cells (pe) attached to Reichert's membrane (r) (**A,B**). Also positive were trophoblastic giant cells (t) (**B**) and endothelial cells (en) lining maternal sinuses (m) (**C,D**). Original magnifications: **A** × 52; **B–D** × 210. Bars: **A** = 100 μm; **B–D** = 20 μm.

described in bovine ON (Bolander et al., 1988). Domain IV in the mouse protein can accommodate 1 Ca^{++}, while Domain I could theoretically bind a maximum of 8 Ca^{++}. We examined the capacity of native SPARC protein for this divalent cation in several ways. Since the small amount of native SPARC available from cell culture precluded reproducible results when we initially measured Ca^{++} binding by equilibrium dialysis, we used a Chelex competitive calcium binding assay. Because of limitations in measuring the dissociation constant and/or the total number of binding sites on a ligand, largely because of different affinities exhibited by the Chelex resin itself for calcium (Waisman and Rasmussen, 1983), we performed experiments in parallel with calmodulin, which has four high-affinity Ca^{++}-binding sites. With this assay, there was a linear relationship between the concentration of calmodulin and nmol of $^{45}Ca^{++}$ bound. We found an average value of 3.8 nmol $^{45}Ca^{++}$ bound per nmol calmodulin (range 3.2–4.9), and 5.3 nmol $^{45}Ca^{++}$ bound per nmol SPARC, under the same experimental conditions. These data indicate that, under conditions in which calmodulin exhibits maximum binding of Ca^{++}, SPARC was associated with a minimum of five Ca^{++} per molecule. This value, which is somewhat lower than the seven Ca^{++} sites calculated for the tissue form of SPARC (Engel et al., 1987), indicates that Domain I has a role in Ca^{++} binding in addition to that contributed by the EF-hand, which provides a single high-affinity site.

Although circular dichroism spectra have been published for the tissue forms of SPARC (ON and BM-40) (Engel et al., 1987;

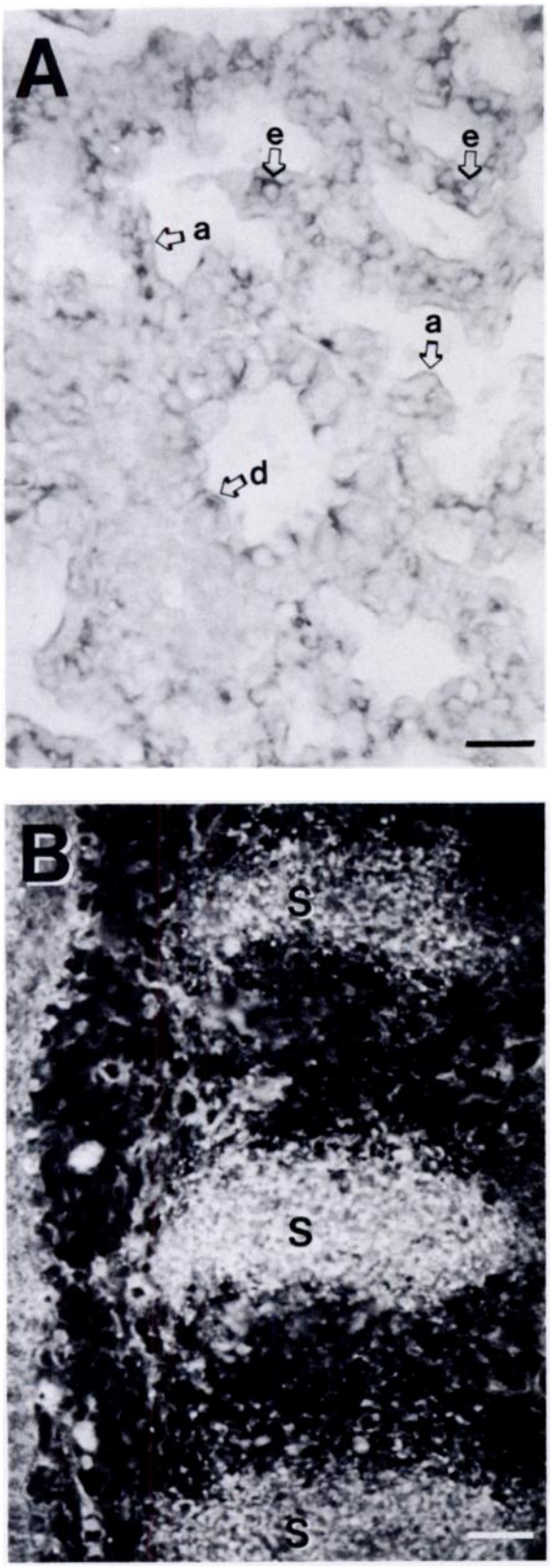

Romberg et al., 1985), their disparity prompted us to examine the structure of the native, intact SPARC molecule secreted from PYS cells. As shown in Figure 7A, SPARC produced a spectrum similar to that shown for intact BM-40 (Engel et al., 1987), with a prominent shoulder at 220 nm. In the presence of 2.5 mM $CaCl_2$ at pH 7.4, the mean residue molar ellipticity calculated for SPARC was -4519 deg·cm^2 dmol^{-1}. This value agrees rather well with that of -5600 deg·cm^2 dmol^{-1} found for BM-40 by Engel et al. (1987), who also reported an α-helical content of 25–30% for the intact molecule. Addition of 12 mM EDTA resulted in a marked decrease in negative ellipticity at 220 nm. Furthermore, a flattened curve with a trough at 205 nm was obtained with denatured SPARC purified on CM-cellulose (data not shown).

A further indication of the Ca^{++}-sensitive nature of SPARC is shown in Figure 7B. In the presence of 4 mM $CaCl_2$, SPARC (S) bound selectively to hydrophobic phenyl–Sepharose and was eluted in the presence of 0.5 M NaCl (lane 2) or 12.5 mM EDTA (lane 3). These results are interesting in light of preliminary studies that demonstrate binding of SPARC to endothelial cells (H. Sage and S. Funk, unpublished observations) and suggest that a hydrophobic surface is exposed when SPARC adopts a native conformation in the presence of Ca^{++}.

Discussion

The distribution of SPARC in mouse tissues can be summarized as follows: (a) in the adult, SPARC was associated with certain epithelia that exhibit high rates of turnover (gut, skin, glandular tissue); (b) SPARC was not detected in adult heart, liver, pancreas, spleen, and kidney; (c) fetal tissues that exhibited high levels of SPARC included thymus, heart, lung, and gut; and (d) in the developing embryo, SPARC expression was particularly enhanced in areas of chondrogenesis, osteogenesis, and somitogenesis. Our studies are in general agreement with the in situ hybridization data published by Hogan and coworkers (Nomura et al., 1988; Holland et al., 1987). The earliest appearance of SPARC mRNA was reported in the 8.5 day mouse embryo (Reichert's membrane, trophoblastic giant cells) (Holland et al., 1987). It was seen in embryonic chondrogenic tissues at day 12 (Table 1), and was rather widely distributed after 13.5 days (Nomura et al., 1988; Mason et al., 1986a) (Table 1).

We note an interesting coincidence between the distribution of SPARC and *fos* mRNA in embryonic mouse bone (Dony and Gruss, 1987). Our data show SPARC protein in the perichondrium/periosteum and in the mesodermal web of the 18-day paw, a tissue that exhibits a rapid proliferative phase at this stage of embryogenesis (Figure 5A). Furthermore, de Togni et al. (1988) showed nuclear staining of *fos* in cartilage of 17-day rat embryos. In newborn mouse bone, SPARC was positive primarily in the zones of

Figure 4. Distribution of SPARC protein in tissues of fetal mouse. Paraffin sections of Bouin's-fixed 18-day fetal lung (**A**) and 14-day fetal thoracic somites (**B**) were exposed to anti-SPARC IgG. The antigen–antibody complex was visualized by the immunoperoxidase technique (**A**) or by RITC indirect immunofluorescence (**B**). Ductal epithelium (d) and alveolar epithelium (a) and endothelium (e) stained positively for SPARC (**A**). Thoracic somites also expressed SPARC, which was seen in the cytoplasm of cells comprising each somite (S) (**B**). Original magnification × 180. Bars = 30 μm.

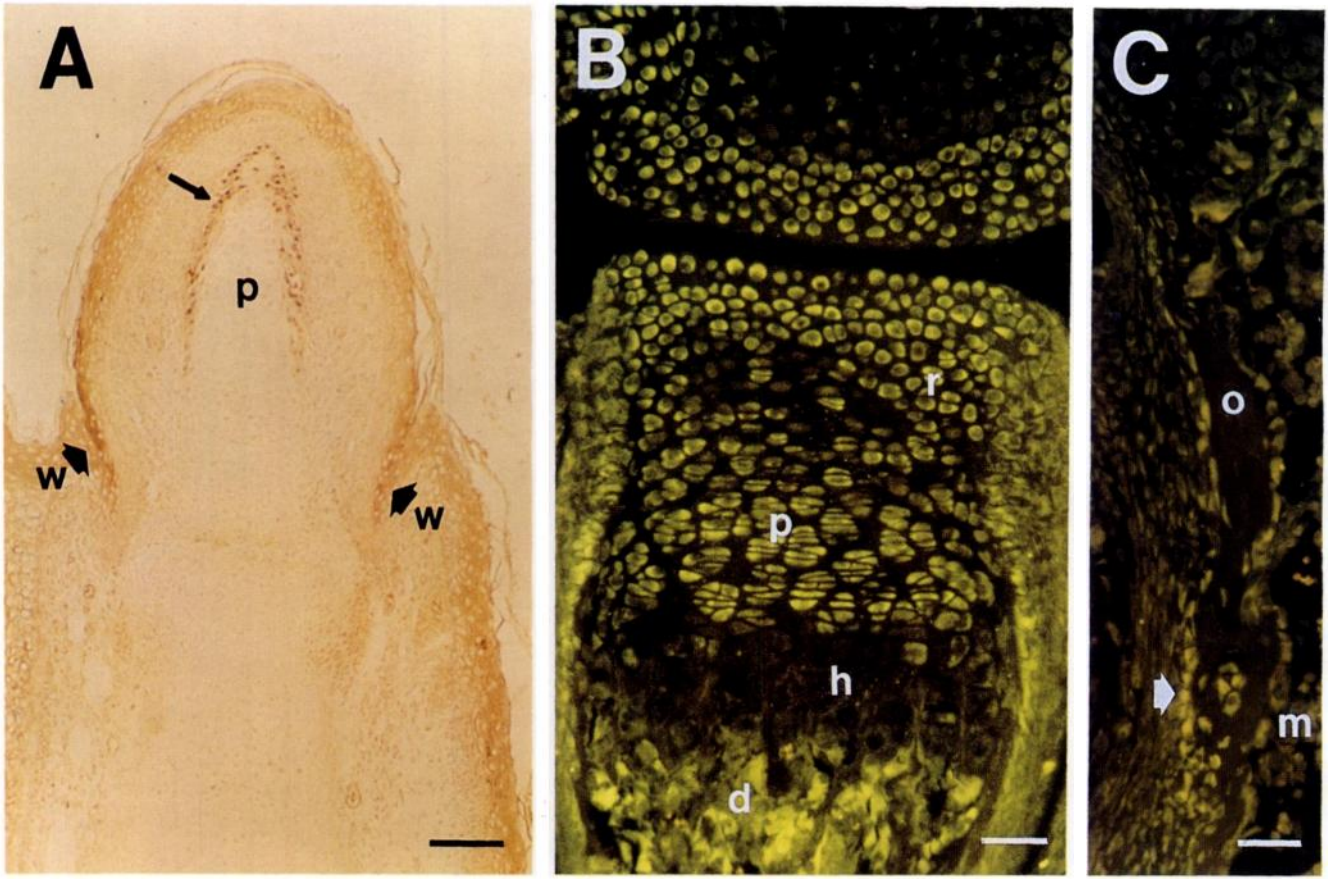

Figure 5. Expression of SPARC protein in developing osseous tissues. Paraffin sections of Bouin's-fixed 18-day fetal mouse forepaw (**A**) and 4–5-day newborn mouse joint (**B,C**) were exposed to anti-SPARC IgG. (**A**) Antigen–antibody complex visualized by the immunoperoxidase technique. (**B,C**) FITC indirect immunofluorescence. In embryonic bone, SPARC was concentrated primarily in the perichondrium/periosteum (arrow) of the phalanx (p), as well as the mesodermal web tissue (w) (**A**). The secondary center of ossification, shown in a carpal epiphysis (**B**), exhibited staining for SPARC in resting chondrocytes (r) as well as those comprising the zones of proliferation (p) and degeneration (d); the hypertrophic zone appeared negative (h). (**C**) Marrow cavity (m) and newly formed osteoid (o) with SPARC-positive osteoblasts (arrow). Original magnifications: **A** × 45; **B,C** × 150. Bars: **A** = 160 μm; **B,C** = 35 μm.

proliferation and degeneration. Nomura et al. (1988) also observed a restricted distribution of SPARC mRNA in 14.5-day periosteum, as well as a more generalized expression in hypertrophic cartilage and in cells associated with bone matrix in later embryos. Although we saw SPARC protein in the hypertrophic zone of fetal mouse bone (not shown), it was conspicuously absent from these chondrocytes in the newborn tissue (Figure 5B). Jundt et al. (1987), in studies of human fracture callus, failed to identify ON (SPARC) in any cartilage except that of "chondroid bone," although ON was present in osteoprogenitor (periosteal) and active osteoblastic cells. We have no explanation for the lack of staining of non-mineralized tissues reported by these investigators. Although there are compelling similarities between the immunohistological distributions of SPARC and TGF-β in mouse embryos (most notably in connective tissues, cartilage, bone, teeth, hair follicles, skin, limb buds, and submandibular gland) (Heine et al., 1987), recent data do not support an induction of SPARC by TGF-β, as suggested by these authors, in the morphogenesis or remodeling of these coincident tissues (Wrana et al., 1988; H. Sage and R. Penttinen, unpublished observations).

Although a function for SPARC (ON) was originally proposed in the mineralization of bone (Termine et al., 1981), Romberg et al. (1985) have shown that this protein inhibits hydroxyapatite formation. Since SPARC is associated with areas of cell proliferation in many tissues, it could function as a general inhibitor of mineralization in all extracellular matrices. As a corollary, SPARC could regulate cellular migration and growth by facilitating the dispersion of, or preventing the formation of, excessive matrix. In this respect, SPARC might resemble the tissue inhibitor of metalloproteinases (TIMP) (Gavrilovic et al., 1987). By neutralizing specific enzymes, TIMP has been proposed to regulate the turnover of the ECM during cell perturbation.

We propose that SPARC might participate in a proliferative response by interacting at the cell surface with other Ca^{+2}-sensitive proteins. Intermolecular regulation is exemplified by the blood clotting proteins, which show calcium-mediated binding to lipids and modulation of protease activity by conformational changes in Ca^{++}-binding domains (Rodgers, 1988). Mellgren (1987) has proposed that cell membranes are preferred sites for Ca-dependent protease action: the protease, a specific inhibitor, and the membrane itself

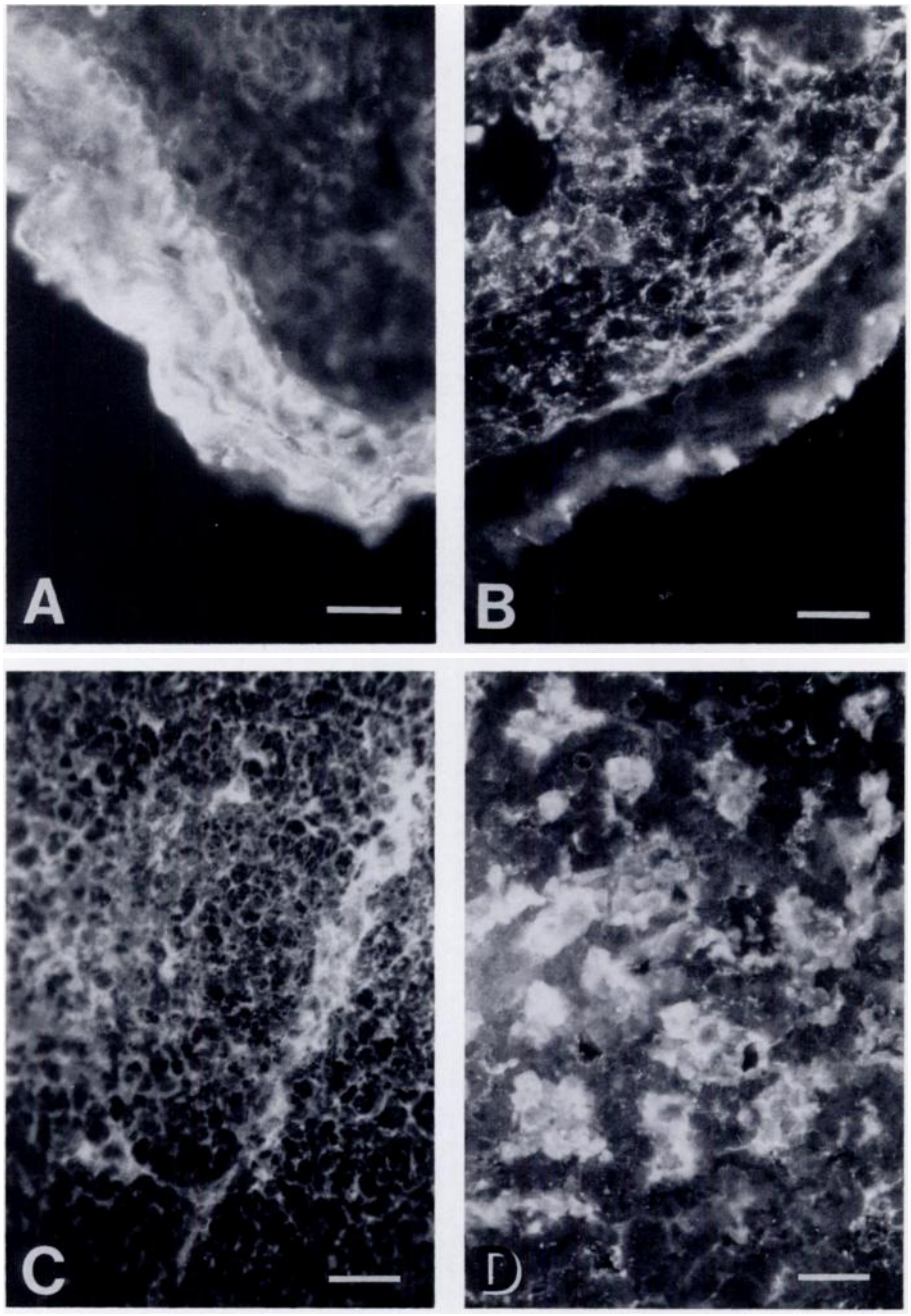

Figure 6. Location of SPARC protein in proliferating epithelia. Frozen sections of newborn mouse skull skin (**A,B**), newborn thymus (**C**), and adult lactating mammary gland (**D**) were exposed to anti-SPARC IgG (**A,C,D**) or to rabbit anti-human FN (**B**), and were visualized by RITC indirect immunofluorescence. In contrast to FN, which was distributed primarily in the dermal interstitium (**B**), SPARC exhibited a preferential localization in the epidermis (**A**). SPARC was also apparent in the epithelial reticular cells of newborn thymic stroma (**C**) and in both ductal and alveolar epithelia of lactating mammary gland (**D**). Original magnification × 180. Bars = 30 μm.

form a regulatory complex which activates membrane-associated protein kinase C after exposure of certain cells to phorbol esters or other mitogens. Transduction of a signal from such an association would lead to the activation of other genes and, indirectly, to cell proliferation. An example of a cell-surface protein that has been claimed to be essential for proliferation of smooth muscle cells is the secreted Ca^{++}-binding protein thrombospondin (Majack et al., 1988).

An analogous example of extracellular protein/matrix regulation of cell growth might be somitogenesis, in which both Ca^{++}-independent and Ca^{++}-dependent mechanisms are operative (Duband et al., 1987). We have observed that SPARC protein was prevalent in 14-day embryo somites and are pursuing the effect of SPARC depletion on cell compaction and dispersion in this system. Since constituents of the plasma membrane and extracellular matrix, such as proteoglycans, can sequester significant levels of Ca^{++}, it is not unreasonable to assume that reservoirs of Ca^{++} could modulate proteins with otherwise high-affinity binding sites. In addition, SPARC might be proteolytically processed in the extracellular space. Excision of the high-affinity EF-hand in vivo could result in an inde-

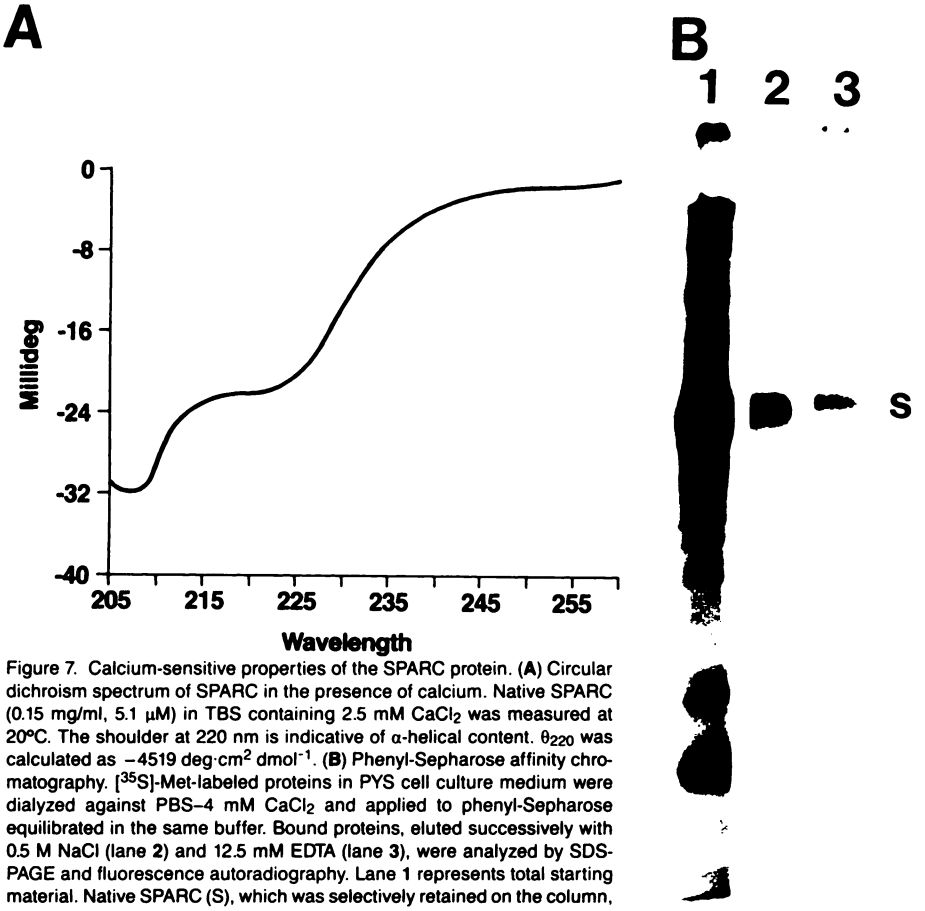

Figure 7. Calcium-sensitive properties of the SPARC protein. (**A**) Circular dichroism spectrum of SPARC in the presence of calcium. Native SPARC (0.15 mg/ml, 5.1 μM) in TBS containing 2.5 mM $CaCl_2$ was measured at 20°C. The shoulder at 220 nm is indicative of α-helical content. θ_{220} was calculated as -4519 deg·cm^2 dmol^{-1}. (**B**) Phenyl-Sepharose affinity chromatography. [^{35}S]-Met-labeled proteins in PYS cell culture medium were dialyzed against PBS–4 mM $CaCl_2$ and applied to phenyl-Sepharose equilibrated in the same buffer. Bound proteins, eluted successively with 0.5 M NaCl (lane 2) and 12.5 mM EDTA (lane 3), were analyzed by SDS-PAGE and fluorescence autoradiography. Lane 1 represents total starting material. Native SPARC (S), which was selectively retained on the column, was dissociated from the hydrophobic resin by salt and/or EDTA. Average recovery from this column was 27%.

pendent function for Domain I with a lower Ca^{++}-binding potential. Alternatively, increased levels of SPARC might disrupt the equilibrium among other secreted proteins to effect the conformational changes necessary for facilitation of cell migration or proliferation.

Acknowledgments

We thank Dr B. Hogan for providing the mouse SPARC cDNA, P. Linnemeyer for histology, Dr R. Klevit and G. Parraga for help with the circular dichroism studies, Dr D. Eyre and S. Apone for performing amino acid analyses, Dr L. Fouser and E. Everitt for preparations of SPARC, and our colleagues in the Departments of Biological Structure and Pathology for discussions and suggestions. Special appreciation is due B. Crockett for preparation of the manuscript.

Literature Cited

Bolander, ME, Young MF, Fisher LW, Yamada U, Termine J (1988): Osteonectin cDNA sequencing reveals potential binding regions for calcium and hydroxyapatite and shows homologies with both a basement membrane protein (SPARC) and a serine protease inhibitor (ovomucoid). Proc Natl Acad Sci USA 85:2919

Davis TN, Urdea MS, Masiarz FR, Thorner J (1986): Isolation of the yeast calmodulin gene: calmodulin is an essential protein. Cell 47:423

de Togni P, Niman H, Raymond V, Sawchenko P, Verma IM (1988): Detection of *fos* protein during osteogenesis by monoclonal antibodies. Mol Cell Biol 8:2251

Dony C, Gruss P (1987): Proto-oncogene c-*fos* expression in growth regions of fetal bone and mesodermal web tissue. Nature 328:711

Duband J-L, Dufour S, Hatta K, Takeichi M, Edelman GM, Thiery JP (1987): Adhesion molecules during somitogenesis in the avian embryo. J Cell Biol 104:1361

Dziadek M, Paulsson M, Aumailley M, Timpl R (1986): Purification and tissue distribution of a small protein (BM-40) extracted from a basement membrane tumor. Eur J Biochem 161:455

Engel J, Taylor W, Paulsson M, Sage H, Hogan B (1987): Calcium-binding domains and calcium-induced transition in SPARC (osteonectin, BM-40), an extracellular glycoprotein expressed in mineralized and nonmineralized tissues. Biochemistry 26:6958

Gavrilovic J, Hembry RM, Reynolds JJ, Murphy G (1987): Tissue inhibitor of metalloproteinases (TIMP) regulates extracellular type I collagen degradation by chondrocytes and endothelial cells. J Cell Sci 87:357

Heine VL, Munoz EF, Flanders KC, Ellingsworth LR, Lam H-YP, Thompson NL, Roberts AB, Sporn MB (1987): Role of transforming growth factor-β in the development of the mouse embryo. J Cell Biol 105:2861

Holland P, Harper S, McVey J, Hogan BLM (1987): *In vivo* expression of

mRNA for the Ca^{++} binding protein SPARC (osteonectin) revealed by *in situ* hybridization. J Cell Biol 105:473

Jundt G, Berghauser K-H, Termine JD, Schulz A (1987): Osteonectin—a differentiation marker of bone cells. Cell Tissue Res 248:409

Laemmli UK (1970): Cleavage of structural proteins during the assembly of the head of bacteriophage T4. Nature 277:680

Majack RA, Goodman LV, Dixit VM (1988): Cell surface thrombospondin is functionally essential for vascular smooth muscle cell proliferation. J Cell Biol 106:415

Mann K, Deutzmann R, Paulsson M, Timpl R (1987): Solubilization of protein BM-40 from a basement membrane tumor with chelating agents and evidence for its identity with osteonectin and SPARC. FEBS Lett 218:167

Mason IJ, Murphy D, Munke M, Francke U, Elliott R, Hogan BLM (1986a): Developmental and transformation-sensitive expression of the SPARC gene on mouse chromosome 11. EMBO J 5:1831

Mason IJ, Taylor A, Williams JG, Sage H, Hogan B (1986b): Evidence from molecular cloning that SPARC, a major product of mouse embryo parietal endoderm, is related to an endothelial cell "culture shock" glycoprotein. EMBO J 5:1465

Mellgren RL (1987): Calcium-dependent proteases: an enzyme system active at cellular membranes? FASEB J 1:110

Nomura S, Wills AJ, Edwards DR, Heath JK, Hogan BLM (1988): Developmental expression of 2ar (osteopontin) and SPARC (osteonectin) RNA as revealed by *in situ* hybridization. J Cell Biol 106:441

Otsuka K, Yao K-L, Wasi S, Tung PS, Aubin JE, Sodek J, Termine JD (1984): Biosynthesis of osteonectin by fetal porcine calvarial cells *in vitro*. J Biol Chem 259:9805

Rodgers GM (1988): Hemostatic properties of normal and perturbed vascular cells. FASEB J 2:116

Romberg RW, Werness PG, Lollar P, Riggs EL, Mann KG (1985): Isolation and characterization of native adult osteonectin. J Biol Chem 260:2728

Sage H (1986a): Culture shock: selective uptake and rapid release of a novel serum protein by endothelial cells *in vitro*. J Biol Chem 261:7082

Sage H (1986b): Characterization and modulation of extracellular glycoproteins secreted by endothelial cells in culture. In Gimbrone M, ed. Contemporary issues in haemostasis and thrombosis. Vol 2. Vascular endothelium in haemostasis and thrombosis. New York, Churchill–Livingstone, 187

Sage H, Decker J, Funk S, Chow M: SPARC: a Ca^{+2}-binding extracellular protein associated with endothelial cell injury and proliferation. J Mol Cell Cardiol, in press

Sage H, Johnson C, Bornstein P (1984): Characterization of a novel serum albumin-binding glycoprotein secreted by endothelial cells in culture. J Biol Chem 259:3993

Sage H, Pritzl P, Bornstein P (1981): Secretory phenotypes of endothelial cells in culture: a comparison of aortic, venous, capillary, and corneal endothelium. Arteriosclerosis 1:427

Sage H, Tupper J, Bramson R (1986): Endothelial cell injury *in vitro* is associated with increased secretion of an M_r 43,000 glycoprotein ligand. J Cell Physiol 127:373

Stenner DD, Tracy RP, Riggs BL, Mann KG (1986): Human platelets contain and secrete osteonectin, a major protein of mineralized bone. Proc Natl Acad Sci USA 83:6892

Termine JD, Kleinman HK, Whitson SW, Conn KM, McGarvey ML, and Martin GR (1981): Osteonectin, a bone-specific protein linking mineral to collagen. Cell 26:99

Tung PS, Domenicucci C, Wasi S, Sodek J (1985): Specific immunohistochemical localization of osteonectin and collagen types I and III in fetal and adult porcine dental tissues. J Histochem Cytochem 33:531

Waisman DM, Khanna NC, Tokuda M (1986): Identification of a major bovine heart Ca^{2+} binding protein. Biochem Biophys Res Commun 139:596

Waisman DM, Rasmussen H (1983): A reexamination of the chelex competitive calcium binding assay. Cell Calcium 4:89

Wasi S, Otsuka K, Yao K-L, Tung PS, Aubin JE, Sodek J, Termine JD (1984): An osteonectin-like protein in porcine periodontal ligament and its synthesis by periodontal ligament fibroblasts. Biochem Cell Biol 62:470

Wrana JL, Maeno M, Hawrylshyn B, Yao K-L, Domenicucci C, Sodek J (1988): Differential effects of transforming growth factor-β on the synthesis of extracellular matrix proteins by normal fetal rat calvarial bone cell populations. J Cell Biol 106:915

Young, MF, Bolander ME, Day AA, Ramis CI, Robey PG, Yamada Y, Termine JD (1986): Osteonectin mRNA: distribution in normal and transformed cells. Nucleic Acids Res 14:4483

Zung P, Domenicucci C, Wasi S, Kuwata F, Sodek J (1986): Osteonectin is a minor component of mineralized connective tissues in rat. Biochem Cell Biol 64:356